Ceramics International 51 (2025) 65512–65523

Contents lists available at ScienceDirect

Ceramics International

journal homepage: www.elsevier.com/locate/ceramint

Sequestration capacity of bio-based ashes and influence of carbonation on the leaching behavior depending on their mineralogical composition

Sara Tominc [a,*], Majda Pavlin [a], Lea Žibret [a], Vilma Ducman [a], Lisbeth M. Ottosen [b]

[a] Laboratory for Cements, Mortars and Ceramics, The Department of Materials, Slovenian National Building and Civil Engineering Institute (ZAG), Dimičeva 12, 1000, Ljubljana, Slovenia

[b] Department of Environmental and Resource Engineering, DTU Sustain, Technical University of Denmark (DTU), Brovej, 2800, Lyngby, Denmark

ARTICLE INFO

Keywords:
Enforced carbonation
Maximum sequestration capacity
Leaching
Heavy metals
Mineralogy
Bio-based ash

ABSTRACT

Mineral CO_2 sequestration is a promising carbon capture and storage approach based on the chemical reaction of CO_2 with alkaline materials containing Ca- and Mg-rich (hydr)oxides and silicates. This results in the formation of relatively insoluble and storable carbonates. This study investigates six ashes of different origins and chemical compositions to assess their CO_2 sequestration potential and leaching behavior, offering insights into their environmental impact and potential risks. The carbonation experiments were conducted under controlled laboratory conditions and the CO_2 sequestration capacity was quantified using a pressure calcimeter, supported by thermogravimetric analysis. Wood ashes and ash from the co-combustion of biomass from a paper mill showed the highest carbonation potential, with CO_2 sequestration capacities between 344.8 and 432.3 g CO_2 per kg of ash and carbonation efficiencies between 82.4 % and 94.4 %. In addition to the high sequestration capacity of the ashes, carbonation was found to affect the leaching behavior of the ash in the environment by changing its mineralogical composition. The process consistently reduced pH and generally decreased the leaching of certain trace elements, except for Mo, and Cr. Nevertheless, the reduction in the leachability of several elements suggests a partial environmental benefit of carbonation. The findings highlight the dual functionality of the carbonation: it provides a viable route for the permanent binding of CO_2 and can enhance the stabilization of industrial residues. However, the persistence of metal leaching indicates that its overall effectiveness in mitigating environmental risks associated with residue disposal or reuse remains material-dependent.

1. Introduction

The CO_2 concentration in the atmosphere has been below 300 ppm for thousands of years [1], while in May 2025, it reached a new record level of 430.51 ppm [2]. CO_2 emissions from the fossil fuel industry play an important role in the accumulation of CO_2 in the atmosphere, as fossil fuel combustion, cement production and other industrial processes release more than 36 Gt of CO_2 worldwide every year [3]. Increasing CO_2 concentrations in the atmosphere are leading to global warming and associated impacts such as rising global temperatures, rising sea levels, ocean acidification and ecosystem disruption [4,5]. These effects emphasize the urgent need to reduce CO_2 and other greenhouse gas emissions. To overcome these challenges, the European Commission adopted the European Green Deal in 2020, which commits the European Union to becoming climate neutral by 2050 [6]. The European Union's initiatives are aimed at various sectors, including the construction industry, transport, and renewable energies. In the first phase, net greenhouse gas emissions are expected to be reduced by at least 55 % by 2030 compared to 1990 levels [6]. In the technological segment related to construction, several technologies are currently being developed or improved which will mainly contribute to the first phase. These include various recycling methods and industrial symbioses such as alkali activation and carbonation (cement/concrete curing with CO_2) as well as carbon capture, utilization and storage (CCUS) technologies [7], which also include mineral sequestration [8,9].

Despite current energy- and cost-intensive carbon capture and storage technologies, mineral CO_2 sequestration represents a straightforward approach that primarily involves the reaction of CO_2 with alkaline materials consisting of Ca- and Mg-rich (hydr)oxides and silicates, leading to the formation of solid carbonate products and their

* Corresponding author.
E-mail addresses: sara.tominc@zag.si (S. Tominc), majda.pavlin@zag.si (M. Pavlin), lea.zibret@zag.si (L. Žibret), vilma.ducman@zag.si (V. Ducman), limo@dtu.dk (L.M. Ottosen).

https://doi.org/10.1016/j.ceramint.2025.11.229
Received 21 July 2025; Received in revised form 13 November 2025; Accepted 17 November 2025
Available online 17 November 2025

subsequent storage [3,10–12]. Many different carbonate phases can be detected in waste materials; from pure Ca-carbonates to Ca-Mg-carbonates and pure Mg-carbonates. However, Ca-containing carbonates are the predominant products after carbonation [13,14]. The reaction between CO_2 and minerals occurs without external energy input [12]. While spontaneous carbonation with atmospheric CO_2 (0.04 %) is generally very slow, carbonation can be enforced by an increased CO_2 concentration or pressure [11,15,16]. Directly binding molecular CO_2 to CaO is a very slow process, and the reaction is faster in the presence of H_2O (liquid or gaseous) [11]. In order to mitigate climate change fast enough, enforced carbonation is highly favorable to natural carbonation. The literature therefore describes a wide range of variations in the curing environment [10,17–23]. The processes of mineral carbonation can be classified as direct or indirect [24]. Indirect mineral carbonation is a multi-stage process in which the metal extraction is separated from the CO_2 reaction and high-purity calcium carbonate is produced, whereas direct mineral carbonation is a single-stage process in which the solid material is treated directly with CO_2 and typically produces carbonated materials for construction and other applications [17,25]. In addition to differences in end products, direct carbonation is generally simpler, less expensive, and more environmentally friendly due to its lower chemicals consumption compared to indirect carbonation [17]. It can be divided into gas-solid, semi-dry (with water vapor) and wet carbonation using liquid water or an alkaline aqueous solution [17,25,26]. Wet carbonation is generally more efficient than gas-solid carbonation under ambient conditions, which makes it attractive for industrial applications. Nevertheless, the main challenges remain, including identification of control mechanisms, optimization of key operating parameters (i.e., liquid/solid (L/S) ratio, CO_2 concentration, pressure, temperature, reagents used) and reducing the high operating costs [12,22,26–28]. In contrast, gas-solid carbonation has been less studied due to its slow reaction rates, which limit large-scale application. However, the performance can be improved by increasing temperature, pressure or CO_2 concentration [12,26]. Semi-dry carbonation offers a balance between dry and wet processes. In this approach, the water is present as vapor, as an adsorbed H_2O layer on the particle surface and in the pores between the particles [17]. This accelerates the reaction kinetics, while significantly less water is required and the slurry system typical of wet carbonation is avoided [29].

Using CO_2 sequestration to produce building materials is an economically sustainable industrial process with negative carbon emissions and therefore deserves attention for further development [30]. The cement industry is the most important sector in which action needs to be taken to reduce greenhouse gas emissions [4]. One promising option is to replace cement in certain applications with alternative binders, such as carbonated steel slag, that are more environmentally friendly [31,32]. Other potential sources for such technology from waste streams are bio-based ashes derived from the combustion of wood biomass residues (e.g. wood chips, pellets, bark), which are typically rich in Ca and/or Mg and can bind CO_2 in the form of stable carbonate compounds [10,18,22]. Carbonation treatment significantly reduces reactive Ca-rich components such as free lime, portlandite, and calcium silicate in waste ash by transforming them into stable carbonate minerals [33]. As a result, carbonated materials can be considered a new class of ceramic-like materials that enhance environmental safety and sustainability. The pH decreases during carbonation, mainly due to the conversion of free lime or periclase into carbonates. However, pH is an important factor influencing the leaching concentration, as potentially toxic elements (PTEs) are leached more under acidic and strongly alkaline conditions [33,34]. Other external factors (e.g. temperature changes, water contact, shape and size of the hardened specimen or monolith, etc.) can also increase the amount of toxic species being released from materials [35,36]. Waste such as biomass ashes may contain elevated concentrations of PTEs [37–40], and immobilization/leaching the potential PTEs should be monitored. Effective waste management strategies require a comprehensive knowledge of how toxic species are immobilized by different materials. The total availability for leaching should be analyzed, which depends on the matrix and mineralogical phases [41] and not by their total content in the solid material [42–44]. Leaching tests are essential for assessing the environmental impact and sustainability of construction materials [45]. The concentration of released toxic species and the legal limits, as defined in national or communal legislation, are needed to estimate the extent of leaching and potential pollution of the studied material/product. Typically the Decree on landfilling waste [46] considering leaching the tests EN 12457/1–4 and EN 14405 is used in the European Union (EU). Some states, e.g. Slovenia, have national decrees on waste aligning with EU regulations such as the Waste Framework Directive and the Landfill Directive [47].

Carbonation treatments can also affect the stability of PTEs by changing the occurrence of minerals in the ash matrix [48,49]. The ash composition also changes during storage and under different environmental conditions, as CO_2 and moisture react with the ash to form carbonates and hydroxides [50]. Carbonation reactions with the formation of $CaCO_3$ lead to a decrease in pH to a less basic value (from ~12 to ~8). This can reduce the solubility of metal hydroxides and increase the stability of heavy metals such as Pb, Zn, and Cu compared to strongly alkaline conditions [51]. The leachability of different PTEs (Pb, Zn, Cu, Cd, Cr and Ni) from untreated and stabilized municipal solid waste incineration fly ash (MSWI-FA) was investigated and related to several factors, such as carbonation mode, different pretreatments, initial moisture content, initial and final pH and various leaching scenarios [48,49]. The pretreatments were able to increase the leaching concentration of PTEs (except Pb), while the leaching concentrations of Cu, Pb and Cr decreased significantly after carbonation [49]. The heavy metals could be solidified by carbonation, and the leaching concentration of some heavy metals in water or acidic solutions decreased. However, Gu et al. [49] found that the leaching concentration of Ni and Zn did not decrease after carbonation, highlighting distinct solidification mechanisms for different heavy metals.

Recently, a method for assessing the CO_2 sequestration potential of waste ashes was proposed [18], revealing that not all ashes are equally suitable. In particular, wood biomass ash (WBA) showed greater sequestration potential than coal ash due to its higher content of Ca oxides and reactive minerals that convert CO_2 into stable carbonates. This finding is particularly important in the context of the circular economy, as about 70 % of WBA still ends up in landfills [10,11,52,53].

In this study, the CO_2 storage capacity of fully carbonated wood biomass and co-combustion ashes was systematically assessed, considering their different origins and properties, with emphasis on how enforced carbonation influences their leaching behavior. While bio-based ashes showed strong potential for permanent CO_2 sequestration, their use is often limited by concerns about the release of toxic elements into the environment. Previous studies have primarily examined either the sequestration capacity of ashes or their leaching characteristics; in this study, both are evaluated simultaneously. However, the interaction between enforced carbonation, CO_2 sequestration capacity, and the environmental mobility of PTEs remains insufficiently understood, particularly for wood and co-combustion ashes. Addressing this gap, this study provides new insights, showing that enforced carbonation not only enhances permanent CO_2 storage but also changes the leaching profile of the ashes. It also highlights the importance of studying the mechanisms affecting the leaching behavior of PTEs, such as Mo and Cr, in carbonated bio-based ashes, and of attempting their immobilization through different treatment methods to ensure their safe utilization.

2. Materials and methods

2.1. Materials

Six types of ash were analyzed: three from wood biomass and three from co-combustion processes. Their characteristics are stated in

Table 1
Characteristics of the investigated ash samples.

Sample ID	Ash Type	Origin	Fuel Type	Combustion method	Combustion temperature (°C)
A1	WB-FA (fly ash)	Danish utility company	Wood chips	Circulating fluidized bed	800–900
A2	WB-FA (fly ash)	Danish utility company	Wood pellets	Grate-fired	up to 1200
A3	WB-BA (bottom ash)	Slovenian heat and power station	Wood chips	Grate-fired	700–900
A4	CCA (bottom ash)	Slovenian paper mill	Paper fiber sludge, wood waste, bark	Circulating fluidized bed	550-650 (primary chamber), 750–900 (secondary chamber)
A5	CCA (bottom ash)	Slovenian combined heat and power station	Brown coal (85 %) and biomass from wood chips (15 %)	Pulverized bed combustion (coal), grate-fired (biomass)	800-900 (biomass), 1000-1300 (coal)
A6	CCA (bottom ash)	Slovenian heat and power station	Municipal waste (light fraction), dehydrated sewage sludge	Grate-fired combustion	650-850 (primary chamber), up to 1200 (secondary chamber)

Table 1. Representative composite samples were provided by the respective companies. The composite samples were obtained by combining several subsamples taken at different sampling points and/or at different operating times to ensure that the analyzed samples are representative of a typical ash production.

2.2. Characterization of ashes

All ash samples were homogenized by quartering, packed in PVC bags, and stored in plastic containers. Prior to chemical analysis, the samples were dried to a constant weight in a laboratory oven at 105 °C and then ground to pass through a 125 μm sieve. To determine the loss on ignition (LOI), the samples were heated at 950 °C following the EN 196–2:2013 standard. Fused beads were prepared by mixing ash with a flux of 50 % lithium tetraborate and 50 % lithium metaborate at a 1:10 ratio (0.947 g of ash to 9.47 g of flux) and heated at 1100 °C. The ash's chemical composition was analyzed using a Thermo Scientific ARL PERFORM'X Wavelength Dispersive X-Ray Fluorescence Spectrometer (WDXRF) equipped with a Rh-Target X-ray tube and the UniQuant software.

For mineralogical analysis, each sample was further sieved to particle sizes below 63 μm and placed in 27-mm holders. X-ray diffraction in the Bragg-Brentano configuration (XRD) was conducted before and after CO_2 exposure using an Empyrean PANalytical X-Ray Diffractometer with a Cu X-ray source, scanned in 0.013° increments from 4° to 70° under clean room conditions. The X-ray tube was operated at 45 kV and 40 mA. The external standard method with corundum (NIST SRM 676a) was used to determine the amorphous amount, and quantification was performed in reference to patterns from the ICDD PDF 4 = 2020 RDB powder diffraction files, using the Rietveld refinement with X'Pert Highscore Plus 4.9 software.

2.3. CO_2 sequestration capacity

Before testing, the ashes were ground and sieved to a particle size below 125 μm, and 20 g of each sample was placed in a closed carbonation chamber for semi-dry carbonation under controlled conditions: relative humidity of (80 ± 3.2) %, temperature of (40 ± 0.5) °C and CO_2 concentration of (4 ± 0.1) vol%. Carbonation was monitored by initially weighing the samples and then weighing them after 3, 7 and 14 days in the chamber. If the difference in weight between the measurements was no more than 0.01 g, the samples were considered fully carbonated. Approximately 2 g of the sample was removed at each weighing, as carbonation was monitored using a pressure calcimeter. The fully carbonated samples were then dried at 105 °C for 24 h for further analysis. The progress of the enforced carbonation process, i.e. the increase in CO_2 content ($CO_{2\ uptake}$, in wt%) in the ash, was determined by calcimetric measurements and calculated using Eq. (1) [54–57], where $CO_{2\ carbonated\ ash}$ (wt%) refers to the measured CO_2 content in the ash after the carbonation treatment and $CO_{2\ original\ ash}$ (wt %) refers to the measured CO_2 content in the original ash.

$$CO_{2\ uptake}(wt\%) = \frac{\left(CO_{2\ carbonated\ ash}\ (wt\%) - CO_{2\ original\ ash}\ (wt\%)\right)}{\left(100 - CO_{2\ carbonated\ ash}\ (wt\%)\right)} \times 100 \quad (1)$$

CO_2 uptake quantifies the actual increase in CO_2 content during the carbonation process, reflecting the real extent of carbonation and indicating the material's reactivity under natural carbonation conditions. In contrast, CO_2 sequestration capacity ($CO_{2\ capacity}$) indicates the total amount of CO_2 that can be sequestered per kilogram of ash (g_{CO2}/kg_{ash}). The experimental CO_2 sequestration capacity of each sample was determined by calcimetric measurements, supported by thermogravimetric analysis (TGA), and calculated using Eq. (2) [33]. The $CO_{2\ carbonated\ ash}$ refers to the measured CO_2 content in the ash (in wt%) after complete carbonation.

$$CO_{2\ capacity\_exp}\left(\frac{g_{CO_2}}{kg_{ash}}\right) = \frac{CO_{2\ carbonated\ ash}\ (wt\%)}{100 - CO_{2\ carbonated\ ash}\ (wt\%)} \times 1000 \quad (2)$$

The experimental CO_2 sequestration capacity was then compared with the theoretical value calculated using the modified Steinour equation (Eq. (3)) [58], which states that oxides such as CaO, MgO, Na_2O, and K_2O can react with CO_2 during the carbonation process, while sulfates and chlorides cannot.

$$CO_{2\ capacity\_th}\left(\frac{g_{CO_2}}{kg_{ash}}\right) = \frac{44}{56} m_{CaO} + \frac{44}{40} m_{MgO} + \frac{44}{62} m_{Na_2O} + \frac{44}{92} m_{K_2O} - \frac{44}{80} m_{SO_3} - \frac{44}{71} m_{Cl} \quad (3)$$

Furthermore, the carbonation efficiency (η) was determined as the ratio of experimental CO_2 sequestration capacity to theoretical CO_2 capacity (Eq. (4)) [58].

$$\eta\ (\%) = \frac{CO_{2\ capacity\_exp}}{CO_{2\ capacity\_th}} \times 100 \quad (4)$$

Calcimetric measurements determine the calcium carbonate and calcium magnesium carbonate (dolomite) content based on their reaction with acid, where the release of CO_2 is measured with a pressure calcimeter (OFITE Calcimeter, OFI Testing Equipment Inc., USA, according to ASTM D 4373). The calcimeter was calibrated before the measurements by reacting HCl with standard $CaCO_3$ (Calcium Carbonate Precipitated, OFI Testing Equipment, Inc, CAS:471-34-1). The calibration curve was generated with five measurements (0.2, 0.4, 0.6, 0.8, and 1.0 g $CaCO_3$) with $R^2 = 0.9996$. Then, 1.0 ± 0.010 g of the dried sample with a particle size below 125 μm was weighed into the reaction cell. The acid cup was filled with 20 mL of 10 % HCl and carefully placed in the reaction cell. After 30 s, the reaction of $CaCO_3$ with HCl generates CO_2, which is measured with a manometer. The amount is calculated using the stoichiometric ratios given in Eq. (5). If the analyzed sample

contains any dolomite ($CaMg(CO_3)_2$), there will be a pause followed by a slow, second rise in pressure. The reaction is complete when the pressure stops increasing, which occurs in 30–40 min. The measurement uncertainty of ±2 % was recently calculated for calcimetric measurements [59].

$$CaCO_3\ (s) + 2HCl\ (aq) \rightarrow CaCl_2\ (aq) + CO_2\ (g) + H_2O\ (l) \quad (5)$$

$$n\ (CaCO_3) = n\ (CO_2) = 1{:}1$$

TGA was performed on dry carbonated samples using a TGA Q5000IR thermal analyzer (TA Instruments, New Castle, Delaware, USA) from 25 to 1000 °C at a heating rate of 10 K min^{-1}. To avoid oxidation, the sample chamber was filled with N_2 at a flow rate of 25 mL min^{-1}. The samples were placed in 100 μL Al_2O_3 crucibles. The CO_2 content (wt%) by TGA was determined by mass loss in the temperature range of decomposition of carbonate minerals (500–900 °C), based on dry matter at 105 °C, as given in Eq. (6). The results were analyzed using TA Universal Analysis 2000 v.4.5A (TA Instruments, New Castle, Delaware, USA). Each sample was tested individually.

$$CO_2(wt\%) = \frac{\Delta m_{500-900\ ^\circ C}}{m_{105\ ^\circ C}} \times 100 \quad (6)$$

2.4. Leaching

The water content was determined as "free water", i.e. water that evaporates after 24 h at 105 °C. The liquid-to-solid (L:S) ratio for the procedure was 1:10, selected from the leaching test EN 12457–2:2002 [60], and the same L:S ratio was chosen for the pH and conductivity measurements. Leaching of the original and carbonated samples was done by suspending ash in distilled water at an L:S ratio of 10 (2.00 g of ash and 20.00 mL of distilled water). After 24 h of agitation, the suspension was filtered and the pH and conductivity were measured. Chloride (Cl^-) and sulfate (SO_2^{2-}) concentrations were measured in the filtrate by ion chromatography (IC) (Thermo Scientific Dionex ICS-1100), the concentrations of As, Ba, Ca, Cu, K, Mg, Na, S, Si, Sr and Zn were measured by inductively coupled plasma optical emission spectroscopy (ICP-OES; Agilent Varian 720-ES) and the concentrations of Cr, Mo, Pb and Sb were measured by inductively coupled plasma mass spectrometry (ICP-MS; Agilent 7850). All samples were acidified before the measurements. Measurements were performed in parallel to ensure reproducibility of results and the average values were used for data analysis.

3. Results and discussion

3.1. Characterization of ashes

First, the characterization of the ash before the carbonation reaction was evaluated. The CaO content in the ash is particularly important as it is crucial for the extent of carbonation [33]. XRF analysis revealed a predominant CaO content of 29–55 wt% together with significant amounts of SiO_2 (6–31 wt%), Al_2O_3 (3–20 wt%), K_2O (0.3–12 wt%), MgO (2–10 wt%) and lower amounts of Fe_2O_3 (1–4 wt%), P_2O_5 (0.3–4 wt%), SO_3 (0–3 wt%), Na_2O (1–2 wt%) and TiO_2 (0–2 wt%). Samples A3 and A4 have the highest CaO content, indicating a strong contribution to the mineralization reaction. The XRF results for primary oxides and LOI at 950 °C are shown in Table 2.

The main crystalline phases in the analyzed samples were Ca- and Mg-containing oxides and silicates, as shown in Fig. 1. The results from XRD pattern evaluation of the original and carbonated ashes are stated in Table 3. The XRD analysis confirmed the presence of calcite as the primary mineral phase in the carbonated samples, varying from 10.1 to 28.4 wt% before carbonation and from 18.7 to 54.5 wt% after carbonation. The main limitation of XRD analysis is that cannot detect amorphous $CaCO_3$ in the sample, but it can distinguish between different $CaCO_3$ polymorphs. Portlandite is the most susceptible phase to carbonation as it reacts very quickly with CO_2 and disappears completely from the XRD patterns, whereas Ca-silicates react only after longer reaction times [55].

Table 3 shows that several mineral phases identified in the untreated ashes (lime, portlandite, periclase, fairchildite) are no longer present in the carbonated ashes. The carbonation products of larnite detected in samples A4 and A6 are metastable $CaCO_3$ polymorphs (aragonite, vaterite), which, according to the literature, later transform into calcite [61] and amorphous C-S-H gel [62]. In sample A2, the amount of hydroxyapatite decreased during carbonation, leading to the formation of monetite, as in Ref. [63]. The main phases contributing to the carbonation process are lime, portlandite, larnite and merwinite [55,57].

3.2. CO_2 sequestration capacity

Given that the CO_2 uptake of these ashes is expected to be certified in the near future [64], ensuring the accuracy and comparability of the measurement results is of utmost importance. As ashes from biomass combustion and co-combustion processes are increasingly recognized for their potential to sequester carbon through mineral carbonation, standardized quantification of their CO_2 uptake capacity is crucial. Variability in ash composition, combustion conditions and exposure environment can significantly affect both the extent and rate of carbonation. Inaccurate or non-comparable data not only hinders scientific understanding, but also undermines environmental accounting, which can lead to inaccurate carbon balance estimates. To minimize inconsistencies, all samples should be fully carbonated prior to analysis, and the selection of appropriate analytical methods is essential, as different techniques can lead to different results. Prior to carbonation, all ashes had undergone some degree of natural carbonation and initially contained calcite as measured by a pressure calcimeter. The CO_2 uptake was calculated after complete carbonation using a pressure calcimeter according to Eq. (1); the results are shown in Table 4 and Fig. 2a. The calculated CO_2 uptake in the ashes ranged from 9.6 to 22.4 wt%, except for sample A6, where the uptake was only 3.3 wt%, as the untreated ash was almost completely carbonated during storage, indicating high reactivity even under ambient conditions. Calcimetric measurements are more reliable for determining CO_2 content, since the main limitation of TGA is the mass overlap with other phases and the small sample size analyzed (10–20 mg for TGA), while 1.0 g of sample is required for calcimetric measurement.

The experimental CO_2 sequestration capacity of the ash was determined using a pressure calcimeter and TGA. The theoretical CO_2 sequestration capacity was calculated from the chemical composition of

Table 2
Loss on ignition (LOI) at 950 °C and chemical composition of the original ashes stated as primary oxides (wt%) by XRF analysis.

ash type:	sample ID	LOI $_{950\ ^\circ C}$	Na_2O	MgO	Al_2O_3	SiO_2	P_2O_5	SO_3	K_2O	CaO	TiO_2	Fe_2O_3	Cl
wood ash	A1	15.13	1.33	4.59	6.22	27.97	2.85	2.59	3.60	31.00	0.19	3.31	0.19
	A2	22.09	0.83	6.80	2.69	9.69	4.18	2.49	11.93	36.62	0.20	0.76	0.00
	A3	26.09	0.48	5.88	3.35	5.64	2.82	2.82	8.14	44.95	0.07	0.68	0.00
co-combustion ash	A4	14.55	0.41	2.12	11.08	14.45	0.26	0.20	0.25	55.40	0.22	0.56	0.00
	A5	12.79	0.57	10.25	7.43	31.17	1.00	0.07	3.21	28.98	0.32	3.56	0.00
	A6	7.21	2.28	3.46	20.05	25.91	2.45	0.86	0.55	28.62	1.85	3.37	0.56

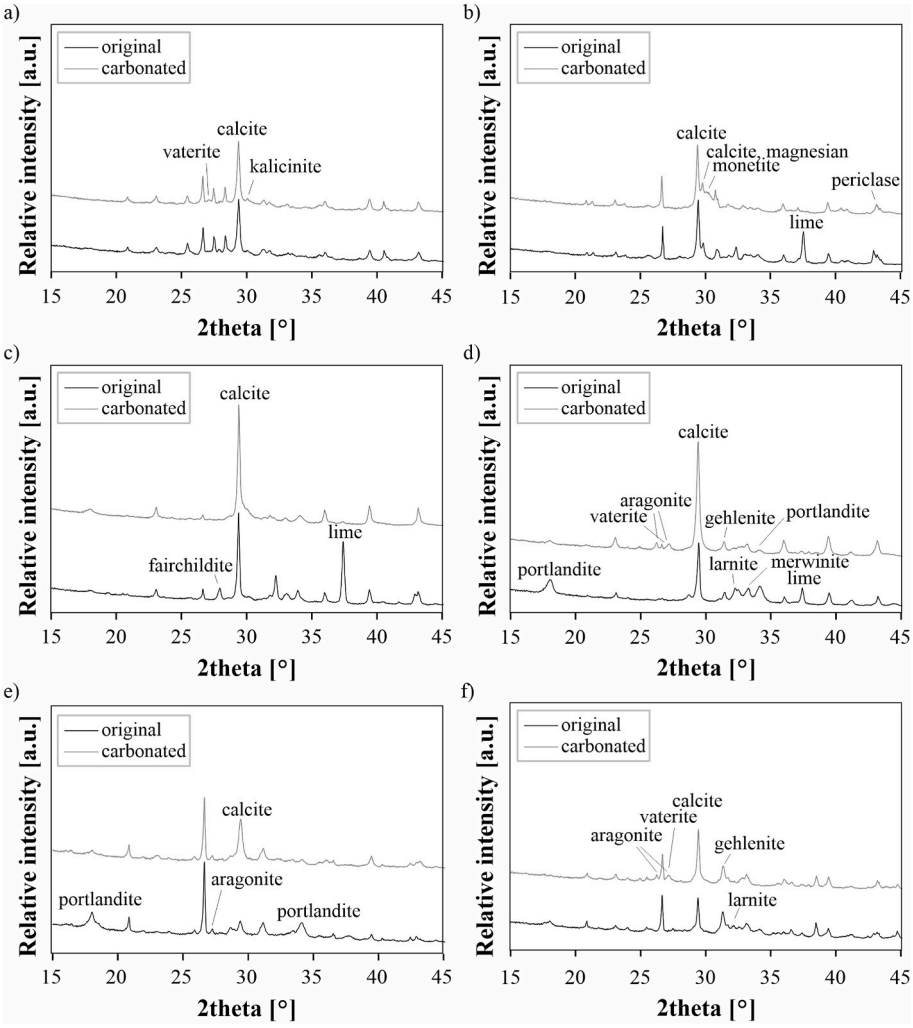

Fig. 1. XRD patterns of powdered original and carbonated ashes. The highest intensity reflections of the main identified phases contributing to carbonation are indicated.

the ashes (XRF results) using the modified Steinour equation (Eq. (3)), as recently reported in the literature [58], and is presented in Table 5 and Fig. 2b. The actual CO_2 sequestration capacity of the samples was slightly lower when determined by TGA compared with calcimetric measurements, as the CO_2 content determined by TGA represents the mass loss resulting from the decomposition of $CaCO_3$ into CaO and CO_2 in the temperature range between 500 °C (shifted to 550 °C for sample A6) and 900 °C [65]. However, for some samples, it may be difficult to determine the correct temperature range if the peaks for carbonate and other decompositions are not clearly separated, so the determination of the range to be analyzed in the thermogram may not be accurate enough. A pressure calcimeter measures carbonate content by the pressure of released CO_2, with the amount of CO_2 calculated using stoichiometric ratios. Furthermore, carbonation efficieny was calculated as the ratio between CO_2 sequestration capacity determined by the pressure calcimeter and the theoretical value, as shown in Table 5.

Samples A2, A3, and A4 have significant potential for carbon sequestration, with CO_2 sequestration capacities ranging from 344.8 g/kg_{ash} to 432.3 g/kg_{ash} according to calcimetric measurements, and high carbonation efficiency ranging from 82.4 % to 94.4 %. The results are comparable to recently reported high values for white slag, which reached a maximum CO_2 sequestration capacity of approximately 360 g_{CO2}/kg_{slag} after a wet carbonation process with pure CO_2, while refractory waste reached a maximum sequestration capacity of 311 g_{CO2}/kg_{slag} [33]. Lin et al. reported a CO_2 sequestration capacity of 536 g/kg for steel slag with direct wet carbonation process and 361 g/kg for blast furnace slag with indirect carbonation, indicating the excellent sequestration properties of these materials [66].

In this study, the CO_2 content in carbonated ash was determined by calcimetric measurements and supported by TGA. Calcimeter and TGA were sufficient to estimate the CO_2 content, as the results differed by less than 3 %. In cases where the deviations are more than 3 %, further analysis with quantitative XRD is recommended to improve the reliability of CO_2 quantification.

Fig. 3 shows the TGA and differential thermogravimetric (DTG) profiles of the samples after complete carbonation. All samples are characterized by four distinct peaks. The first two peaks, which start at about 25 °C and end at about 200 °C (region I), are attributed to surface-bound water (the first peak), while the second peak is related to dihydroxylation of the mineral phase or possibly to partial decarbonation of the bicarbonates, according to Ref. [67]. The third peak, observed between 250 and 500 °C (region II), can be attributed to several thermal processes [68]. It may result from the burnout of organic carbon at 250–500 °C or from the decomposition of portlandite between 400 and 500 °C [65,68]. However, no portlandite was detected by XRD in the analyzed samples after carbonation treatment. In addition, $MgCO_3$ can also decompose in the temperature range between 300 and 500 °C [69], but its presence cannot be reliably confirmed by XRD, as the main peak (100 % intensity at 32.8°) is weak and overlaps with those of fairchildite, hydroxylapatite, or K-carbonate. The last peak results from the

Table 3
XRD results of the original (orig) and carbonated (carb) ash samples determined using the Rietveld refinement. The corresponding agreement indices Weighted R profile (Rwp) and Goodness of fit (GOF) are stated to indicate the refinement validity. The precision of XRD analysis is approximately ±2 wt%.

Phase	Formula	A1		A2		A3		A4		A5		A6	
		orig	carb	orig	carb	orig	carb	orig	carb	orig	carb	orig	carb
calcite	$CaCO_3$	21.3	25.0	23.1	54.5	28.4	57.5	24.8	50.4	10.1	24.4	11.8	18.7
dolomite	$CaMg(CO_3)_2$									8.1	8.7		
kalicinite	$KHCO_3$	<1.0	1.6										
K-carbonate γ	K_2CO_3					1.1	2.0						
aragonite	$CaCO_3$								7.0	1.2	<1.0		7.0
vaterite	$CaCO_3$	<1.0	<1.0						1.7				2.0
fairchildite	$K_2Ca(CO_3)_2$					9.0	<1.0						
lime	CaO			8.0	<1.0	17.2	<1.0	4.1	<1.0	<1.0	0.0		
periclase	MgO			4.5	<1.0	4.3	<1.0			<1.0	<1.0	1.3	0.0
portlandite	$Ca(OH)_2$			1.0	<1.0	<1.0	<1.0	19.1	<1.0	13.9	<1.0	1.1	0.0
quartz	SiO_2	3.9	4.4	4.1	3.8	1.3	<1.0			10.5	9.4	6.4	4.8
merwinite	$Ca_3Mg(SiO_4)_2$							12.3	1.0				
melilite	$Ca_2(Al,Mg,Fe)(Al,Si,B)SiO_7)$											7.4	6.7
plagioclase	$NaAlSi_3O_8$ – $CaAl_2Si_2O_8$	1.7	1.4										
microcline	$KAlSi_3O_8$	7.7	8.0										
gehlenite	$Ca_2Al[AlSiO_7]$							6.3	4.4			2.8	4.0
mayenite	$Ca_{12}Al_{14}O_{33}$					<1.0	<1.0	1.5	<1.0			<1.0	<1.0
larnite	Ca_2SiO_4							13.8	8.9			26.1	1.3
anhydrite	$CaSO_4$	2.2	1.6									<1.0	<1.0
arcanite	K_2SO_4			8.7	7.2								
apatite	$Ca_5(PO_4)_3(F,Cl,OH)$	<1.0	<1.0			1.1	1.3						
hydroxy-apatite	$Ca_5(PO_4)_3OH$			11.0	7.4								
monetite	$CaHPO_4$				2.6								
sylvine	KCl	2.6	2.1										
Al	Al											2.9	1.8
amorphous content		57.2	60.1	39.0	23.7	35.2	35.5	18.1	25.7	54.5	55.1	37.3	51.2
Rwp		4.4	4.5	5.3	3.5	4.4	4.6	4.0	4.2	4.4	4.6	3.7	3.4
GOF		2.7	2.8	3.0	2.0	2.5	2.6	2.2	2.4	2.8	3.0	2.3	2.2

Table 4
CO_2 uptake (in wt%) based on the CO_2 content in the original and carbonated sample, determined with the pressure calcimeter.

Sample ID		Calcimeter			CO_2 uptake
		$CaCO_3$ (wt%)	$CaMg(CO_3)_2$ (wt%)	CO_2 (wt%)	(wt%)
A1	orig	20.7	0.1	9.1	–
	carb	38.4	0.5	17.1	9.6
A2	orig	29.4	0.0	12.9	–
	carb	58.1	0.2	25.6	17.1
A3	orig	42.7	1.1	19.3	–
	carb	67.8	0.8	30.2	15.6
A4	orig	24.9	0.9	11.4	–
	carb	61.3	1.3	27.6	22.4
A5	orig	11.9	2.3	6.3	–
	carb	34.4	1.7	15.9	11.4
A6	orig	21.2	0.0	9.3	–
	carb	27.9	0.0	12.3	3.3

decomposition of carbonates and their transformation into more stable phases, usually occurring between 500 and 900 °C (region III) [65], except for sample A6, where the peak is shifted to 550 °C. The mass loss in the region from approximately 500 °C–800 °C can be attributed to calcite decomposition, while the mass loss around 800 °C may result from K_2CO_3 decomposition [68]. However, the presence of K_2CO_3 cannot be reliably confirmed by XRD, as the main peak (100 % intensity at 31.3°) is weak and overlaps with those of calcite and kalicinite.

3.3. Environmental behavior

The leaching behavior of untreated and carbonated ashes prepared according to EN 12457–2:2002 is compared in Fig. 4, where the carbonated ashes show decreased pH values and conductivities. These differences can be attributed to the mineralogical changes during carbonation [55]. At the maximum sequestration capacity achieved for sample A3, the corresponding pH was 10.1 (decreased from 12.7). Maintaining an optimal pH is crucial for increasing the sequestration

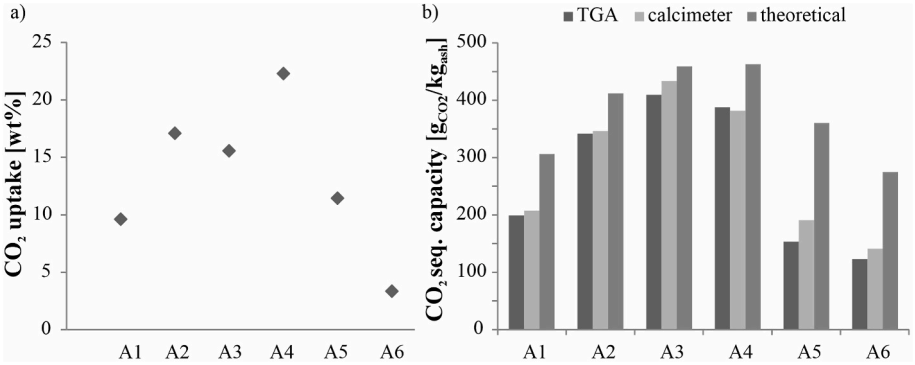

Fig. 2. a) CO_2 uptake (in wt%), determined with a pressure calcimeter and b) comparison of CO_2 sequestration capacity (in g_{CO2}/kg_{ash}) determined by pressure calcimeter and TGA.

Table 5
CO_2 content (in wt%) after complete carbonation and the CO_2 sequestration capacity (in g_{CO2}/kg_{ash}), determined by TGA and calcimetry. The temperature range for sample A6 is shifted to 550–900 °C. Theoretical CO_2 sequestration capacity (in g_{CO2}/kg_{ash}) was calculated using the modified Steinour equation, and carbonation efficiency was determined using calcimetric measurements as the experimental CO_2 sequestration capacity value.

Sample ID	TGA (wt.%)		TGA calculations		Calcimetric calculations	CO_2 capacity_exp (TGA)	CO_2 capacity_exp (calcimeter)	CO_2 capacity_th (Steinour)	η
	25–105 °C	500–900 °C	$m_{105\ °C}$	CO_2 (wt %)	CO_2 (wt%)	(g_{CO2}/kg_{ash})	(g_{CO2}/kg_{ash})	(g_{CO2}/kg_{ash})	%
A1	1.4	16.3	98.6	16.5	17.1	**197.8**	**206.2**	**304.8**	**67.7**
A2	2.6	24.7	97.4	25.4	25.6	**340.1**	**344.8**	**410.5**	**84.0**
A3	3.2	28.1	96.8	29.0	30.2	**408.3**	**432.2**	**457.6**	**94.4**
A4	1.0	27.6	99.0	27.9	27.6	**386.4**	**380.3**	**461.5**	**82.4**
A5	1.0	13.1	99.0	13.2	15.9	**152.4**	**189.7**	**359.0**	**52.8**
A6	1.4	10.7	98.6	10.9	12.3	**122.0**	**139.8**	**273.4**	**51.1**

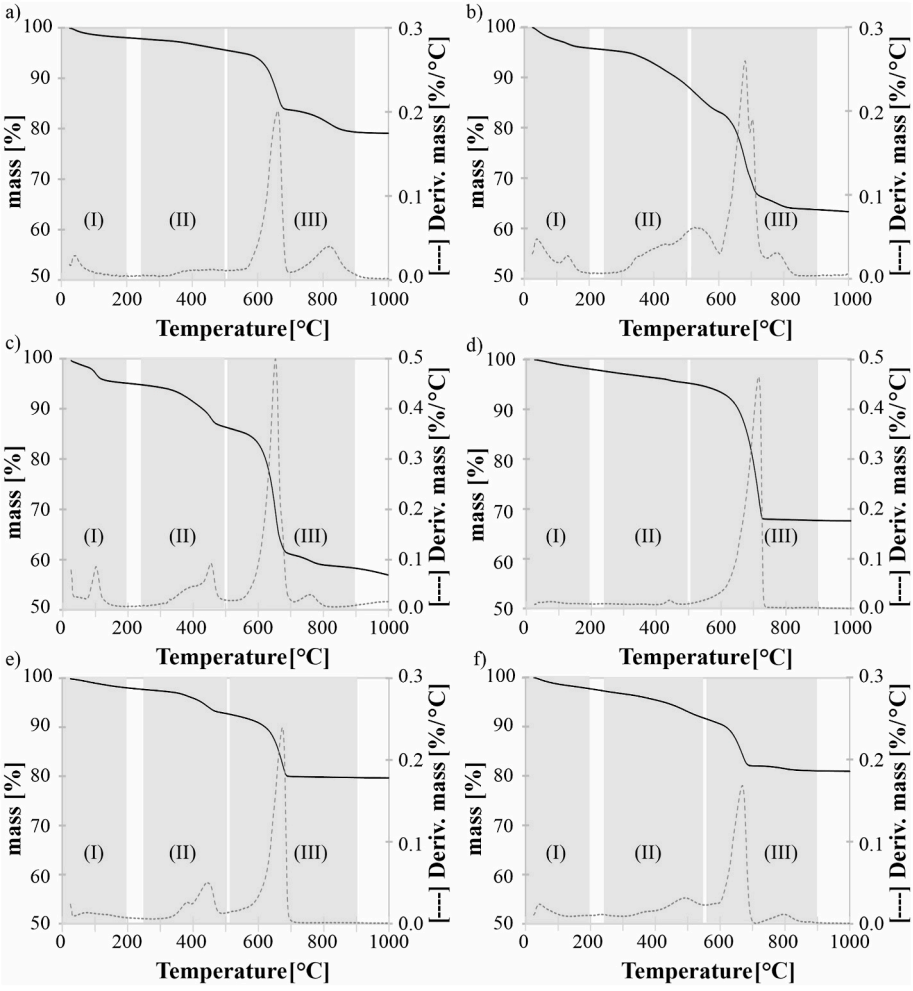

Fig. 3. TGA and DTG curves of sample a) A1, b) A2, c) A3, d) A4, e) A5 and f) A6 after full carbonation.

efficiency [33]. The high content of Ca or Mg oxides contributed to the high basicity of the ashes [55]: the initial pH of the untreated samples was remarkably high (between 11.2 and 12.7), while the pH decreased to between 8.9 and 11.1 after carbonation, as shown in Fig. 4a. The alkalinity of an ash depends on its content of carbonates and hydroxides [50]. Fig. 4b shows that the conductivity in samples A1-A3 is significantly higher than in samples A4-A6, indicating the presence of more soluble species, especially in samples A2 and A3.

Leaching results for major elements and anions are shown in Fig. 5. The Ca concentration in the leachates decreases in all samples because carbonation leads to the formation of less water-soluble phases [70]. As shown in Fig. 5, the leaching of Ca was reduced in all samples after enforced carbonation, due to the formation of calcite and other less soluble Ca compounds. Sample A6 shows only a slight decrease in Ca concentration, while the Ca concentration in sample A1 has decreased significantly in the leachate. Even after carbonation, the Ca concentration in A1 remains the highest among all analyzed samples, as it showed only a slight increase in calcite content during carbonation according to the XRD results in Table 3. A significant increase in calcite was observed in samples A2, A3 and A4, which in turn show a low Ca concentration in their leachates. The leachates of samples A4 and A6 show a decreased Ca content after carbonation, but the concentration is still higher than in

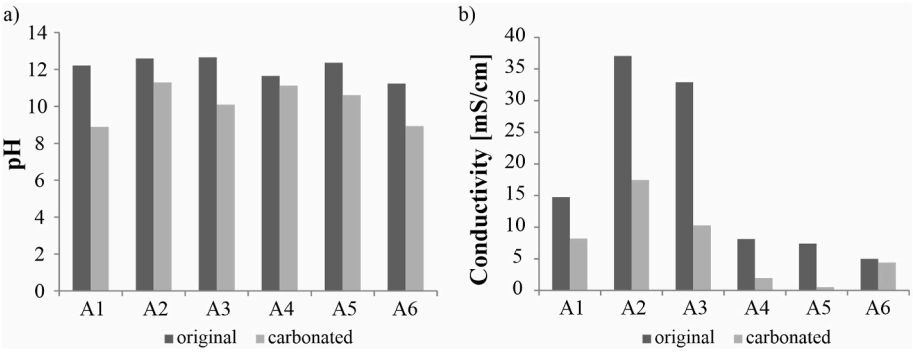

Fig. 4. Leaching behavior of the original and carbonated ashes: a) pH of the leachates and b) conductivity.

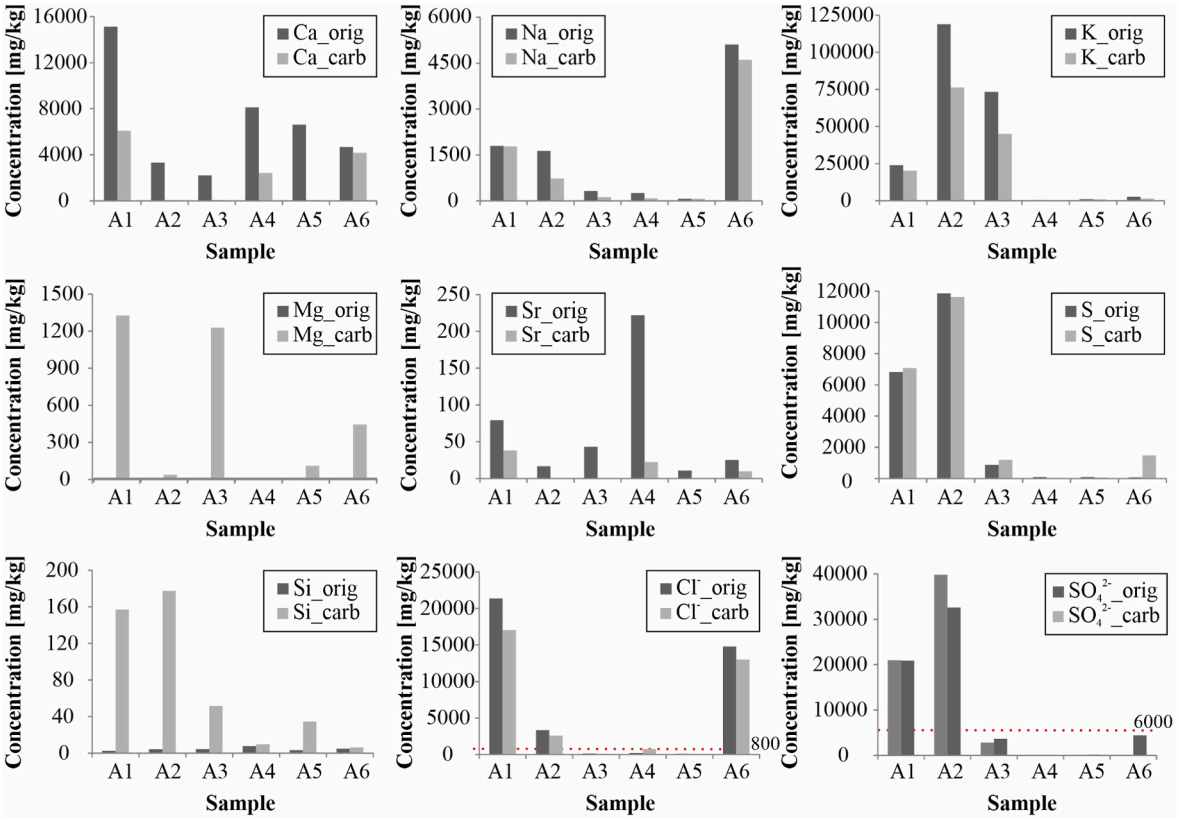

Fig. 5. Concentrations of major elements and anions derived from the leaching test (EN 12457–2:2002) performed on the original and carbonated ashes. Dotted lines highlight the permissible limits for inert waste in the Decree on waste landfilling [46].

samples A2, A3 and A5. Hence, partially soluble minerals/compounds were formed in samples A4 and A6 after carbonation, which are a source of Ca in the leachates.

The enforced carbonation increased CO_2 uptake, leading to the formation of $CaCO_3$ from reactive phases such as lime and portlandite. High amounts of portlandite were found in the original samples A4 and A5, which were probably converted to $CaCO_3$ after carbonation. Portlandite can also react with silica in the amorphous phase to form calcium silicate hydrates (C-S-H) [71]. Based on mineralogical information about the quartz present in the samples, the relative quartz content decreases slightly in all samples during carbonation, except for sample A1, where it increases.

Larnite was identified in the original ashes A4 and A6. Merwinite (a Ca-Mg silicate) was also found in the original ash A4. The carbonation reaction proceeds faster for larnite than for merwinite, as Mg substitution in merwinite negatively affects carbonation reactivity and alters the products from calcite to Mg-calcite, aragonite, and magnesite [72]. Table 3 shows that the transformation of merwinite is almost complete after carbonation, while 8.9 wt% larnite is still present in sample A4. The hydration of mayenite can contribute to the formation of portlandite and subsequently to the formation of $CaCO_3$ [73,74]. Although mayenite was identified as a mineral phase capable of carbonation, its carbonation and contribution to $CaCO_3$ formation in the present work is low. It is difficult to determine the amount of this phase more precisely, as 1.5 wt% and less than 1 wt% before carbonation and less than 1 wt% after carbonation were identified in samples A3, A4 and A6, respectively.

Amorphous content in the samples was determined by Rietveld refinement. In samples A4 and A6, an increase in amorphous content after carbonation was observed (7.6 % and 13.9 %, respectively),

possibly due to the formation of amorphous calcium aluminum silicates and/or amorphous $CaCO_3$, especially in sample A6, where a significant increase in amorphous content was measured. This increase in amorphous content might also be related to the leaching of Ca from both samples. The $CaCO_3$ polymorphs aragonite and vaterite were also identified in both samples.

The relative K concentration decreased slightly during carbonation due to mass gain from carbonation, but leachate concentrations were significantly higher in the wood ashes (A1, A2, and A3) than in the co-combustion ashes (A4, A5, and A6). The XRF data in Table 2 show that A2 has the highest K content, followed by A3 and A1. In ashes, K predominantly occurs as soluble salts in the form of sulfates, chlorides, and carbonates [75]. In sample A1, sylvine and kalicinite can contribute to K leaching before and after accelerated carbonation. Sylvine can also contribute to Cl^- leaching. In sample A2, arcanite may be responsible for the leaching of K and SO_4^{2-}. After carbonation, the arcanite content decreases, resulting in less leaching. The hydration and carbonation processes lead to a hard, dense structure that decreases K leaching [76]. In sample A3, fairchildite was detected, a mineral phase that occurs in biomass ash and can transform into calcite after enforced carbonation [77].

A low concentration of Mg (<0.3 mg/kg) was measured in all leachates from the original samples. In samples A2, A3, A5 and A6, Mg is present as periclase, while no periclase was found in samples A1 and A4. Merwinite was also determined as an Mg-containing mineral in sample A4, while dolomite and brucite were found in A5. Through hydration, periclase may form Mg-hydroxide, which can then be carbonated to various hydrated Mg-carbonates [78,79]. However, it was observed that in some samples (A2, A3, A5, and A6), reducing the amount of periclase and converting it to a more soluble Mg compound could increase the Mg leaching after carbonation.

Si concentrations in leachates increased with the degree of carbonation and decreasing pH [55]. Sample A2 has the highest Si concentration after carbonation, followed by A1. The increased leachability of Si may result from the solubility of amorphous SiO_2, the decomposition or transformation of silicates to $CaCO_3$ in amorphous Ca-Al silicates [75] (in sample A2), and the dissolution of newly formed silicate phases from various alumino-silicates (e.g., in sample A1, plagioclase, microcline). The leaching of sulfur and sulfate shows a consistent leaching pattern, with relatively high concentrations in the leachates of A1 and A2 and lower concentrations in A3 and A6. In A1, sulfate leaching could be due to the dissolution of anhydrite (based on Rietveld analysis). Based on the XRD results (Table 3), anhydrite is the mineral phase responsible for sulfate (SO_4^{2-}) and Ca leaching. The pH in sample A1 after carbonation is 8.9 (Fig. 3), while in sample A2 after carbonation it is 11.3, which is a significant difference considering that both samples were exposed to the same carbonation conditions. The higher sulfate leaching could result from the progressive dissolution of ettringite due to the carbonation process [75]; however, no ettringite was detected in our samples. In sample A2, arcanite is possibly the major contributor to the leaching of sulfate ions, whereas in samples A3 and A6, the sulfate concentration is much lower and identifying the mineral phase contributing to the leaching is difficult.

Chlorine (Cl^-) with high concentrations in the leachate before and after carbonation treatment was measured in the leachates of samples A1 and A6. A much lower concentration was detected in sample A2, while the concentrations in the other samples were below the limit values for inert waste [46]. The chlorine content in samples A1, A2 and A6 decreases after carbonation. Based on the Rietveld refinement data, sylvine is the main mineral phase contributing to leaching in sample A1, while no chlorine-containing mineral phase is present in samples A2 and A6 (Fig. 4). Sample A4 is the only sample where the concentration of Cl^- is higher after carbonation. Based on the XRF data (Table 2), chlorine was found in samples A1 and A6 at concentrations of less than 1 wt% (A1: 0.19 wt%, A6: 0.56 wt%). Since the chlorine concentration in the leachate of sample A1 is higher and the total concentration in sample A1 is lower than in sample A6, the chemical compound present in sample A6 could have lower solubility.

Previous studies have shown that mineralization plays a fundamental role in preventing the leaching of heavy metals [33,70,80]. Wood fly ashes (WFAs) generally contain higher concentrations of heavy metals than wood biomass bottom ashes (WBBAs) [70]. Therefore, we compared two WFAs (A1 and A2) with one WBBA (A3), all in the particle size fraction of less than 0.125 mm in diameter. The heavy metal concentrations in all WBAs are below the limits for agricultural and forestry applications set by various European countries, as reported by Carević et al. [81]. There is no direct correlation between the composition of toxic metals in biomass ashes and the amount of PTEs in leachates [42–44]. The reduction in leaching of PTEs after carbonation was not clearly due to a reduced pH, but may have resulted from the formation of insoluble metal carbonates reacting with dissolved CO_2 [71].

Fig. 6 shows the results of leaching before and after enforced carbonation for various PTEs, including Ba, Cu, Mo, Pb, Sb, As, Zn and Cr. The results indicate that Cu, Pb, Sb and As leaching are below the limits specified in the Decree on the waste landfill for inert waste [46] in all samples. For Zn, only sample A2 (original) exceeded the leaching limits. After carbonation, the Zn concentration in sample A2 decreased significantly to below the limit value. In general, the concentrations of Zn are low in all samples. Ottosen et al. [70] recently developed the "In Projections to Latent Structures (PLS) model", which shows that the leaching of Zn is strongly dependent on K concentration and the leaching of SO_4^{2-}. Supporting this finding, the Zn concentration was highest in WFA (A2), which also had the highest K concentration and the highest concentration of soluble SO_4^{2-}. Carbonation leads to a decrease in pH (Fig. 4), and changes in pH may cause a higher solubility of Pb [82]. Pb can be entrapped by carbonates, as the leaching concentrations decreased after carbonation in all samples. Other metal-containing minerals, such as oxides, phosphates and sulfates of Pb, were also identified in MSWI bottom ashes and can occur in the analyzed ashes [83]. The Ba concentration decreased significantly after carbonation and was below the legal limit in all samples. A high pH enables the formation of $BaCO_3$ from $BaCl_2$ [84]. According to Librandi et al. [55], Ba is originally bound to Ca-silicates and is probably released from these phases together with Ca during carbonation, although this behavior was not directly confirmed in our study.

The leaching of Cr prior to hydration/carbonation is negatively correlated with the leaching of Ca, as shown in Figs. 5 and 6. The decreased Cr leaching may be related to the hydration/carbonation of CaO to $CaCO_3$, but the continued leaching suggests that some Cr remains in compounds unaffected by hydration/carbonation or in newly formed soluble phases containing Cr (as described in Ref. [70]). The mobility of toxic metals in WFA depends on the properties of the ash [70]. During the hydration/carbonation processes, the leaching of the most toxic elements, including Cr, decreased; however, as shown in Fig. 6, the decrease is small in samples A1, A2 and A3. Oxyanions such as CrO_4^{2-} and MoO_4^{2-} are mobile at high pH values [85], and especially in sample A2, where the pH decreases only slightly according to Fig. 4, the leaching concentrations of Cr and Mo did not change significantly. Due to the toxicity of Cr(VI), which is present in aqueous solutions in various forms at different pH values, more attention needs to be paid to leachable Cr [86].

Sb leaching concentrations did not exceed limit values in any samples, regardless of whether they were carbonated (Fig. 6). A slight increase after carbonation was observed in all samples except for sample A6. The dissolution of Ca antimonates (romeite) controls Sb leaching in the ash at pH 8–11. Since Ca is preferentially leached, Ca-rich structures become less soluble at higher pH values. The solubility of Sb depends on pH and Ca^{2+}. Enforced carbonation can only reduce Sb leaching if a lower pH is achieved, which allows Sb to adsorb onto Fe and Al oxides. Adsorption on hydrous Fe oxides and not on amorphous Al minerals controls Sb leaching at pH < 9 in MSWI bottom ashes [87]. However, in the current ashes, Fe oxides were not identified (see Table 3), so such

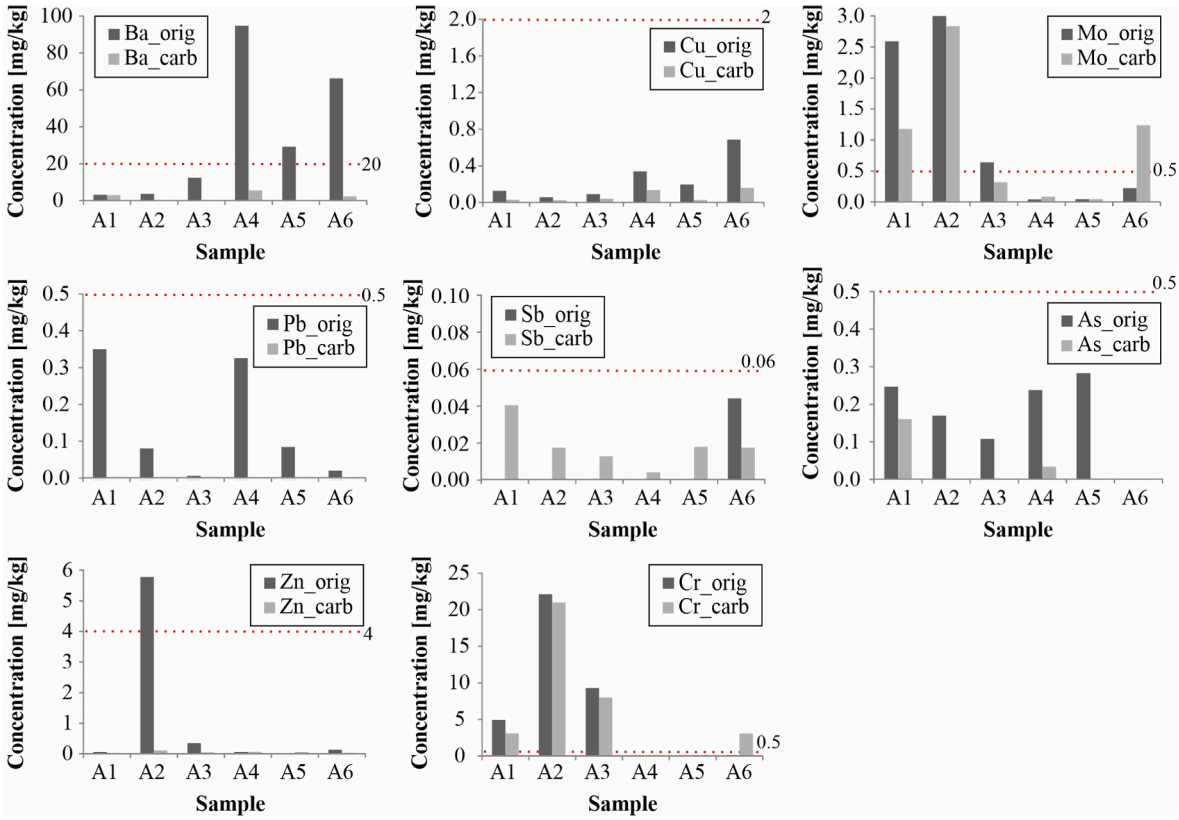

Fig. 6. Concentrations of PTEs derived from the leaching test (EN 12457–2:2002) performed on the original and carbonated ashes. Dotted lines highlight the permissible limits for inert waste in the Decree on waste landfilling [46].

adsorption may not occur, as indicated by the increase in Sb leaching in A1 and A6 with a pH in this range after carbonation (Fig. 6).

4. Conclusions

This study shows that carbonation reactions under semi-dry conditions can be completed within 14 days for different ash types, with CO_2 uptake largely dependent on the initial carbonation state of the materials. Complete carbonation of samples before testing and the use of appropriate analytical techniques are key to obtaining consistent results. Wood fly ash, wood bottom ash and ash from co-combusted biomass showed remarkable CO_2 sequestration capacities of 344.8 g_{CO2}/kg_{ash} (A2), 432.3 g_{CO2}/kg_{ash} (A3) and 380.3 g_{CO2}/kg_{ash} (A4), which are comparable to or even exceed the values of some industrial slags. Carbonation efficiencies also reached high values for these samples: 84.0 % (A2), 94.4 % (A3), and 82.4 % (A4).

Enforced carbonation increased CO_2 uptake, lowered pH, and led to mineralogical changes that influenced leaching behavior. While the leaching of Zn, Ba, As and Pb decreased in all samples, the leaching of Cr and Mo increased in sample A6, which originates from the co-combustion of municipal waste and dehydrated sewage sludge. In wood ashes (A1-A3), Cr and Mo concentrations only slightly decreased and remain above the permissible limit for inert waste, while concentrations of Sb slightly increased after carbonation but did not exceed limit values in any sample. Carbonation can promote the stabilization of bio-based ashes through partial immobilization of hazardous elements, but the continued leaching of certain metals shows that its overall environmental effectiveness remains limited and should be evaluated on a case-by-case basis.

Future studies should assess the long-term stability of carbonated ash and investigate its applications in construction materials (e.g., alkali-activated materials) or agriculture. Extending research to a wider range of ash types and mixed materials could reveal new opportunities for carbon sequestration; however, emphasis should also be placed on developing processes and technologies that enhance the immobilization of toxic metals.

CRediT authorship contribution statement

Sara Tominc: Writing – review & editing, Writing – original draft, Methodology, Investigation, Conceptualization. **Majda Pavlin:** Writing – review & editing, Writing – original draft, Investigation. **Lea Žibret:** Writing – review & editing, Writing – original draft, Investigation. **Vilma Ducman:** Writing – review & editing, Supervision, Methodology, Funding acquisition, Conceptualization. **Lisbeth M. Ottosen:** Writing – review & editing, Conceptualization.

Data availability statement

The data presented in this study are openly available in the DiRROS repository at http://hdl.handle.net/20.500.12556/DiRROS-23902 and are also available upon request from the corresponding author.

Funding

This research was EU-funded by Horizon Europe ASHCYCLE project, grants number 101058162 and partially supported by the Slovenian Research and Innovation Agency (ARIS) under research core grant no. P2-0273.

Declaration of competing interest

The authors declare that they have no known competing financial interests or personal relationships that could have appeared to influence the work reported in this paper.

Acknowledgments

The authors would like to thank Ebba Cederberg Schnell from DTU for IC, ICP-OES and ICP-MS measurements.

References

[1] F. Pacheco-Torgal, 1-Introduction to carbon dioxide sequestration-based cementitious construction materials, in: Carbon Dioxide Sequestration in Cementitious Construction Materials, Woodhead Publishing, 2018, pp. 3–12, https://doi.org/10.1016/B978-0-08-102444-7.00001-0.
[2] Carbon dioxide | vital signs – climate change: vital signs of the planet. https://climate.nasa.gov/vital-signs/carbon-dioxide/.
[3] A. Alturki, The global carbon footprint and how new carbon mineralization technologies can be used to reduce CO_2 emissions, ChemEngineering 44 (6) (2022), https://doi.org/10.3390/chemengineering6030044.
[4] S.K. Kaliyavaradhan, T.-C. Ling, Potential of CO_2 sequestration through construction and demolition (C & D) waste — an overview, J. CO2 Util. 20 (2017) 234–242, https://doi.org/10.1016/j.jcou.2017.05.014.
[5] P.A. K, et al., Impact of climate change and anthropogenic activities on aquatic ecosystem – a review, Environ. Res. 238 (Dec. 2023) 117233, https://doi.org/10.1016/J.ENVRES.2023.117233.
[6] European Commission, The European green deal. https://commission.europa.eu/strategy-and-policy/priorities-2019-2024/european-green-deal_en.
[7] L. Miu, Public perceptions of CCUS in central and Eastern Europe – implications for community engagement, Balt. Carbon Forum 2 (2023) 6–7, https://doi.org/10.21595/bcf.2023.23580.
[8] C.M. Woodall, N. McQueen, H. Pilorgé, J. Wilcox, Utilization of mineral carbonation products: current state and potential, Greenh. Gases Sci. Technol. 9 (6) (2019) 1096–1113, https://doi.org/10.1002/ghg.1940.
[9] A. Uliasz-Bocheńczyk, A comprehensive review of CO_2 mineral sequestration methods using coal fly ash for carbon capture, utilisation, and storage (CCUS) technology, Energies 17 (22) (2024) 5605, https://doi.org/10.3390/en17225605.
[10] R. Koch, G. Sailer, S. Paczkowski, S. Pelz, J. Poetsch, J. Müller, Lab-scale carbonation of wood ash for CO_2-Sequestration, Energies 14 (21) (2021) 7371, https://doi.org/10.3390/en14217371.
[11] L. Li, M. Wu, An overview of utilizing CO_2 for accelerated carbonation treatment in the concrete industry, J. CO2 Util. 60 (2022) 102000, https://doi.org/10.1016/j.jcou.2022.102000.
[12] R.K. Saran, V. Arora, S. Yadav, CO_2 sequestration by mineral carbonation: a review, Glob. Nest J. 20 (3) (2018) 497–503, https://doi.org/10.30955/gnj.002597.
[13] R.M. Santos, J. Van Bouwel, E. Vandevelde, G. Mertens, J. Elsen, T. Van Gerven, Accelerated mineral carbonation of stainless steel slags for CO_2 storage and waste valorization: effect of process parameters on geochemical properties, Int. J. Greenh. Gas Control 17 (2013) 32–45, https://doi.org/10.1016/j.ijggc.2013.04.004.
[14] X. Wang, W. Ni, J. Li, S. Zhang, K. Li, Study on mineral compositions of direct carbonated steel slag by QXRD, TG, FTIR, and XPS, Energies 14 (15) (2021), https://doi.org/10.3390/en14154489.
[15] W. Ashraf, Carbonation of cement-based materials: challenges and opportunities, Constr. Build. Mater. 120 (2016) 558–570, https://doi.org/10.1016/j.conbuildmat.2016.05.080.
[16] S.O. Ekolu, A review on effects of curing, sheltering, and CO_2 concentration upon natural carbonation of concrete, Constr. Build. Mater. 127 (2016) 306–320, https://doi.org/10.1016/j.conbuildmat.2016.09.056.
[17] M. Zajac, J. Skibsted, F. Bullerjahn, J. Skocek, Semi-dry carbonation of recycled concrete paste, J. CO2 Util. 63 (2022) 102111, https://doi.org/10.1016/j.jcou.2022.102111.
[18] S. Tominc, V. Ducman, Methodology for evaluating the CO_2 sequestration capacity of waste ashes, Materials 16 (15) (2023) 5284, https://doi.org/10.3390/ma16155284.
[19] R. Infante Gomes, C. Brazão Farinha, R. Veiga, J. de Brito, P. Faria, D. Bastos, CO_2 sequestration by construction and demolition waste aggregates and effect on mortars and concrete performance - an overview, Renew. Sustain. Energy Rev. 152 (2021) 111668, https://doi.org/10.1016/j.rser.2021.111668.
[20] M. Quaghebeur, P. Nielsen, L. Horckmans, D. Van Mechelen, Accelerated carbonation of steel slag compacts: development of high-strength construction materials, Front. Energy Res. 3 (2015), https://doi.org/10.3389/fenrg.2015.00052.
[21] R.R. Tamilselvi Dananjayan, P. Kandasamy, R. Andimuthu, Direct mineral carbonation of coal fly ash for CO_2 sequestration, J. Clean. Prod. 112 (2016) 4173–4182, https://doi.org/10.1016/j.jclepro.2015.05.145.
[22] F. Winnefeld, A. Leemann, A. German, B. Lothenbach, CO_2 storage in cement and concrete by mineral carbonation, Curr. Opin. Green Sustainable Chem. 38 (2022) 100672, https://doi.org/10.1016/j.cogsc.2022.100672.
[23] H.C. Gomes, E.D. Reis, R.C. de Azevedo, C. de, S. Rodrigues, F.S.J. Poggiali, Carbonation of aggregates from construction and demolition waste applied to concrete: a review, Buildings 13 (4) (2023) 1097, https://doi.org/10.3390/buildings13041097.
[24] H. Bobicki, Q. Liu, Z. Xu, H. Zeng, Carbon capture and storage using alkaline industrial wastes, Prog. Energy Combust. Sci. 38 (2) (2012) 302–320, https://doi.org/10.1016/j.pecs.2011.11.002.
[25] R. Snellings, et al., Rilem TC recommendation RILEM TC 309 - MCP : recommendation on terminology for mineral carbonation construction products, Mater. Struct. 58 (2025) 57, https://doi.org/10.1617/s11527-024-02467-y.
[26] W. Liu, et al., CO_2 sequestration by direct gas–solid carbonation of fly ash with steam addition, J. Clean. Prod. 178 (2018) 98–107, https://doi.org/10.1016/j.jclepro.2017.12.281.
[27] D. Medas, G. Cappai, G. De Giudici, M. Piredda, S. Podda, Accelerated carbonation by cement kiln dust in aqueous slurries: chemical and mineralogical investigation, Greenh. Gases Sci. Technol. 7 (4) (2017) 692–705, https://doi.org/10.1002/ghg.1681.
[28] S.P. Veetil, M. Hitch, Recent developments and challenges of aqueous mineral carbonation: a review, Int. J. Environ. Sci. Technol. 17 (10) (2020) 4359–4380, https://doi.org/10.1007/s13762-020-02776-z.
[29] Y. Fang, J. Shan, Q. Wang, M. Zhao, X. Sun, Semi-dry and aqueous carbonation of steel slag: characteristics and properties of steel slag as supplementary cementitious materials, Constr. Build. Mater. 425 (2024) 135981, https://doi.org/10.1016/j.conbuildmat.2024.135981.
[30] N. Lippiatt, T.C. Ling, S.Y. Pan, Towards carbon-neutral construction materials: carbonation of cement-based materials and the future perspective, J. Build. Eng. 28 (2020) 101062, https://doi.org/10.1016/j.jobe.2019.101062.
[31] H.K. Kamyab, P. Nielsen, P. Van Mierloo, L. Horckmans, Carbstone pavers: a sustainable solution for the urban environment, Appl. Sci. 11 (14) (2021), https://doi.org/10.3390/app11146418.
[32] First footpath constructed with Carbstone clinkers | VITO. https://vito.be/en/news/first-footpath-constructed-carbstone-clinkers.
[33] S. Capelo-Avilés, et al., A thorough assessment of mineral carbonation of steel slag and refractory waste, J. CO2 Util. 82 (2024) 102770, https://doi.org/10.1016/j.jcou.2024.102770.
[34] T. Sicong, J. Jianguo, Z. Chang, Influence of flue gas SO_2 on the toxicity of heavy metals in municipal solid waste incinerator fly ash after accelerated carbonation stabilization, J. Hazard. Mater. 192 (3) (2011) 1609–1615, https://doi.org/10.1016/j.jhazmat.2011.06.085.
[35] H.A. van der Sloot, A. van Zomeren, J.C.L. Meeussen, P. Seignette, R. Bleijerveld, Test method selection, validation against field data, and predictive modelling for impact evaluation of stabilised waste disposal, J. Hazard. Mater. 141 (2007) 354–369, https://doi.org/10.1016/j.jhazmat.2006.05.106.
[36] W.J.J. Huijgen, R.N.J. Comans, Carbonation of steel slag for CO_2 sequestration: leaching of products and reaction mechanisms, Environ. Sci. Technol. 40 (8) (2006) 2790–2796, https://doi.org/10.1021/es052534b.
[37] J. Zhai, I.T. Burke, D.I. Stewart, Beneficial management of biomass combustion ashes, Renew. Sustain. Energy Rev. 151 (2021) 111555, https://doi.org/10.1016/j.rser.2021.111555.
[38] N.C. Cruz, F.C. Silva, L.A.C. Tarelho, S.M. Rodrigues, Critical review of key variables affecting potential recycling applications of ash produced at large-scale biomass combustion plants, Resour. Conserv. Recycl. 150 (2019) 104427, https://doi.org/10.1016/j.resconrec.2019.104427.
[39] S.V. Vassilev, C.G. Vassileva, D. Baxter, Trace element concentrations and associations in some biomass ashes, Fuel 129 (2014) 292–313, https://doi.org/10.1016/j.fuel.2014.04.001.
[40] H. Luo, Y. Cheng, D. He, E.-H. Yang, Review of leaching behavior of municipal solid waste incineration (MSWI) ash, Sci. Total Environ. 668 (2019) 90–103, https://doi.org/10.1016/j.scitotenv.2019.03.004.
[41] A. Coz, B. Ruiz-Labrador, R. Alonso-Santurde, M. Coronado, A. Andres, Leaching behaviour methodology as a tool for stabilised/solidified metallic waste characterisation. https://www.researchgate.net/publication/259357933_Leaching_behaviour_methodology_as_a_tool_for_stabilisedsolidified_metallic_waste_characterisation.
[42] J.J. Dijkstra, H.A. van der Sloot, R.N.J. Comans, The leaching of major and trace elements from MSWI bottom ash as a function of pH and time, Appl. Geochem. 21 (2) (2006) 335–351, https://doi.org/10.1016/j.apgeochem.2005.11.003.
[43] D.S. Kosson, H.A. van der Sloot, F. Sanchez, A.C. Garrabrants, An integrated framework for evaluating leaching in waste management and utilization of secondary materials, Environ. Eng. Sci. 19 (3) (2002) 159–204.
[44] H.A. van der Sloot, L. Heasman, P. Quevauviller, M.J.A. van den Berg, Harmonization of leaching/extraction Tests, Elsevier, 1997.
[45] M. Cabrera, A.P. Galvín, F. Agrela, 12 - Leaching issues in recycled aggregate concrete, in: R.C. Agrela (Ed.), Woodhead Publishing Series in Civil and Structural Engineering, Woodhead Publishing, 2019, pp. 329–356, https://doi.org/10.1016/B978-0-08-102480-5.00012-9.
[46] Official gazette of republic Slovenia, decree on waste landfill, nos, 10/14, 54/15, 36/16, 37/18," 2014, https://www.ecolex.org/details/legislation/decree-on-the-landfill-of-waste-lex-faoc130542/, 2020.
[47] Official gazette of republic Slovenia, decree on waste, Nos. 37/15, 69/15, 129/20 and 77/22. https://www.uradni-list.si/1/objava.jsp?sop=2021-01-0302, 2022.
[48] W. Li, et al., Stability evaluation of potentially toxic elements in MSWI fly ash during carbonation in view of two leaching scenarios, Sci. Total Environ. 803 (2022) 150135, https://doi.org/10.1016/j.scitotenv.2021.150135.
[49] Q. Gu, T. Wang, W. Wu, D. Wang, B. Jin, Influence of pretreatments on accelerated dry carbonation of MSWI fly ash under medium temperatures, Chem. Eng. J. 414 (2021) 128756, https://doi.org/10.1016/j.cej.2021.128756.
[50] L. Etiégni, A.G. Campbell, Physical and chemical characteristics of wood ash, Bioresour. Technol. 37 (2) (1991) 173–178, https://doi.org/10.1016/0960-8524(91)90207-Z.
[51] J.M. Chimenos, A.I. Fernández, R. Nadal, F. Espiell, Short-term natural weathering of MSWI bottom ash, J. Hazard. Mater. 79 (3) (2000) 287–299, https://doi.org/10.1016/S0304-3894(00)00270-3.

[52] N. Tripathi, C.D. Hills, R.S. Singh, J.S. Singh, Offsetting anthropogenic carbon emissions from biomass waste and mineralised carbon dioxide, Sci. Rep. 10 (1) (2020) 1–9, https://doi.org/10.1038/s41598-020-57801-5.
[53] N. Ukrainczyk, N. Vrbos, E.A.B. Koenders, Reuse of woody biomass ash waste in cementitious materials, Chem. Biochem. Eng. Q. 30 (2) (2016) 137–148, https://doi.org/10.15255/CABEQ.2015.2231.
[54] G. Ferrara, P. Humbert, D. Garufi, P. Palmero, Evolution of CO_2 uptake degree of ordinary Portland cement during accelerated aqueous mineralisation, Ceramics 7 (4) (2024) 1711–1726, https://doi.org/10.3390/ceramics7040109.
[55] P. Librandi, P. Nielsen, G. Costa, R. Snellings, M. Quaghebeur, R. Baciocchi, Mechanical and environmental properties of carbonated steel slag compacts as a function of mineralogy and CO_2 uptake, J. CO2 Util. 33 (2019) 201–214, https://doi.org/10.1016/j.jcou.2019.05.028.
[56] F. Bonfante, P. Humbert, J.M. Tulliani, P. Palmero, G. Ferrara, CO_2 uptake of cement by-pass dust via direct aqueous carbonation: an experimental design for time and temperature optimisation, Mater. Struct. Constr. 57 (8) (2024) 1–18, https://doi.org/10.1617/s11527-024-02457-0.
[57] P. Nielsen, M. Quaghebeur, Determination of the CO_2 uptake of construction products manufactured by mineral carbonation, Minerals 13 (8) (2023), https://doi.org/10.3390/min13081079.
[58] J. Chen, et al., A novel insight into CO_2-cured cement modified by ultrasonic carbonated waste incineration fly ash: mechanical properties , carbon sequestration, and heavy metals immobilization, Carbon Capture Sci. Technol. 14 (2025) 100368, https://doi.org/10.1016/j.ccst.2025.100368.
[59] N. Kavčič, S. Tominc, L. Zibret, G. Zibret, M. Kolar, V. Ducman, Comparing methods for determining the CO_2 content in CO_2-Sequestering materials and natural rock, Ceram. Int. 51 (25) (2025) 43786–43795, https://doi.org/10.1016/j.ceramint.2025.07.109.
[60] EN 12457-2:2004: Characterisation of waste - Leaching - Compliance test for leaching of granular waste materials and sludges - Part 2: One stage batch test at a liquid to solid ratio of 10 l/kg for materials with particle size below 4 mm (without or with size reduction).
[61] A. Pondelak, F. Rosi, C. Maurich, C. Miliani, S.D. Škapin, A. Sever Škapin, The role of relative humidity on crystallization of calcium carbonate from calcium acetoacetate precursor, Appl. Surf. Sci. 506 (2020) 144768, https://doi.org/10.1016/j.apsusc.2019.144768.
[62] O. Shtepenko, C. Hills, A. Brough, M. Thomas, The effect of carbon dioxide on β-dicalcium silicate and Portland cement, Chem. Eng. J. 118 (1–2) (2006) 107–118, https://doi.org/10.1016/j.cej.2006.02.005.
[63] A.M. Kaushal, V.R. Vangala, R. Suryanarayanan, Unusual effect of water vapor pressure on dehydration of dibasic calcium phosphate dihydrate, J. Pharm. Sci. 100 (2011) 1456–1466, https://doi.org/10.1002/jps.22372.
[64] European Union, PE-CONS 92/1/24 REV 1 Regulation Of The European Parliament And Of The Council Establishing A Union Certification Framework For Permanent Carbon Removals, Carbon Farming And Carbon Storage In Products. https://data.consilium.europa.eu/doc/document/PE-92-2024-REV-1/en/pdf.
[65] S.V. Vassilev, C.G. Vassileva, N.L. Petrova, Mineral carbonation of biomass ashes in relation to their CO_2 capture and storage potential, ACS Omega 6 (22) (2021) 14598–14611, https://doi.org/10.1021/acsomega.1c01730.
[66] X. Lin, Y. Zhang, H. Liu, G. Boczkaj, Y. Cao, C. Wang, Carbon dioxide sequestration by industrial wastes through mineral carbonation: current status and perspectives, J. Clean. Prod. 434 (2024) 140258, https://doi.org/10.1016/j.jclepro.2023.140258.
[67] S.V. Vassilev, C.G. Vassileva, N.L. Petrova, Thermal behaviour of biomass ashes in air and inert atmosphere with respect to their decarbonation, Fuel 314 (2022) 122766, https://doi.org/10.1016/j.fuel.2021.122766.
[68] M. Protić, A. Miltojević, B. Zoraja, M. Raos, I. Krstić, Application of thermogravimetry for determination of carbon content in biomass ash as an indicator of the efficiency of the combustion process, Teh. Vjesn. 28 (5) (2021) 1762–1768, https://doi.org/10.17559/TV-20200508110940.
[69] J. Eichermüller, K. Handke, A. Kappler, H. Thorwarth, Comparison of methods for quantifying the carbon content of carbonated wood ash, Chem.-Ing.-Tech. (0) (2025) 1–8, https://doi.org/10.1002/cite.70015.
[70] L.M. Ottosen, N.M. Sigvardsen, Heavy metal leaching from wood ash before and after hydration and carbonation, Environ. Sci. Pollut. Res. (2024), https://doi.org/10.1007/s11356-024-33221-0.
[71] R.J. Yeo, et al., Strategies for heavy metals immobilization in municipal solid waste incineration bottom ash: a critical review, Rev. Environ. Sci. Bio/Technology 23 (2024) 503–568, https://doi.org/10.1007/S11157-024-09694-3.
[72] S. Zhang, et al., The carbonation and hardening properties of larnite, åkermanite and merwinite in steel slag: a study from experiments and DFT calculations, J. Ind. Eng. Chem. (2024), https://doi.org/10.1016/j.jiec.2024.12.040.
[73] J.H. Kim, W.T. Kwon, Semi-dry carbonation process using fly ash from solid refused fuel power plant, Sustain. Times 11 (3) (2019) 908, https://doi.org/10.3390/SU11030908.
[74] G. Hoschek, Gehlenite stability in the system $CaO-Al_2O_3-SiO_2-H_2O-CO_2$, Contrib. Mineral. Petrol. 47 (1974) 245–254, https://doi.org/10.1007/BF00390149/METRICS.
[75] A. Astrup T, A. Munton, i A. Polettin, R. Pomi, T. Van Gerven, Van Zomeren, Chapter 24 - treatment and reuse of incineration bottom ash, in: Environmental Materials and Waste, Elsevier Inc., 2016, pp. 607–645, https://doi.org/10.1016/B978-0-12-803837-6.00024-X.
[76] B.-M. Steenari, L.G. Karlsson, O. Lindqvist, Evaluation of the leaching characteristics of wood ash and the influence of ash agglomeration, Biomass Bioenergy 16 (2) (1999) 119–136, https://doi.org/10.1016/S0961-9534(98)00070-1.
[77] M.J.F. Llorente, J.M.M. Laplaza, R.E. Cuadrado, J.E.C. García, Ash behaviour of lignocellulosic biomass in bubbling fluidised bed combustion, Fuel 85 (9) (2006) 1157–1165, https://doi.org/10.1016/j.fuel.2005.11.019.
[78] S.A. Walling, J.L. Provis, Magnesia-based cements: A journey of 150 years, and cements for the future? Chem. Rev. 116 (7) (2016) 4170–4204, https://doi.org/10.1021/acs.chemrev.5b00463.
[79] S. Ma, A.H. Akca, D. Esposito, S. Kawashima, Influence of aqueous carbonate species on hydration and carbonation of reactive MgO cement, J. CO2 Util. 41 (2020) 101260, https://doi.org/10.1016/j.jcou.2020.101260.
[80] S. Hajji, T. Turki, A. Boubakri, M. Ben Amor, N. Mzoughi, Study of cadmium adsorption onto calcite using full factorial experiment design, Desalination Water Treat. 83 (2017) 222–233, https://doi.org/10.5004/dwt.2017.21079.
[81] I. Carević, N. Štirmer, M. Trkmić, K.K. Jurić, Leaching characteristics of wood biomass fly ash cement composites, Appl. Sci. 10 (8704) (2020) 1–17, https://doi.org/10.3390/app10238704.
[82] J. Todorovic, H. Ecke, Demobilisation of critical contaminants in four typical waste-to-energy ashes by carbonation, Waste Manag. 26 (4) (2006) 430–441, https://doi.org/10.1016/j.wasman.2005.11.011.
[83] P. Freyssinet, et al., Chemical changes and leachate mass balance of municipal solid waste bottom ash submitted to weathering, Waste Manag. 22 (2) (2002) 159–172, https://doi.org/10.1016/S0956-053X(01)00065-4.
[84] S. Park, J.-H. Bang, K. Song, C.W. Jeon, J. Park, Barium carbonate precipitation as a method to fix and utilize carbon dioxide, Chem. Eng. J. 284 (2016) 1251–1258, https://doi.org/10.1016/j.cej.2015.09.059.
[85] M. Chrysochoou, D. Dermatas, Evaluation of ettringite and hydrocalumite formation for heavy metal immobilization: literature review and experimental study, J. Hazard. Mater. 136 (1) (2006) 20–33, https://doi.org/10.1016/J.JHAZMAT.2005.11.008.
[86] J. Ščančar, R. Milačič, A critical overview of Cr speciation analysis based on high performance liquid chromatography and spectrometric techniques, J. Anal. At. Spectrom. 29 (3) (2014) 427–443, https://doi.org/10.1039/C3JA50198A.
[87] G. Cornelis, T. Van Gerven, C. Vandecasteele, Antimony leaching from uncarbonated and carbonated MSWI bottom ash, J. Hazard. Mater. 137 (3) (2006) 1284–1292, https://doi.org/10.1016/j.jhazmat.2006.04.048.